EUROPEAN ORGANIZATION FOR NUCLEAR RESEARCH

CERN-EP/84-31
13 March 1984

AN UPGRADED CONFIGURATION OF A HIGH- LUMINOSITY SPECTROMETER FOR DEEP-INELASTIC MUON SCATTERING EXPERIMENTS

Bologna–CERN–Dubna–Munich–Saclay Collaboration

A.C. Benvenuti, D. Bollini, G. Bruni, T. Camporesi,
G. Heiman, G. Laurenti, L. Monari and F.L. Navarria

Istituto di Fisica dell'Università and INFN, Bologna, Italy

A. Argento, W. Birr, K. Deiters, M. Goossens, F. Nanni, L. Piemontese and A. Staude

CERN, Geneva, Switzerland

I.A. Golutvin, V.Y. Karzhavin, M.Y. Kazarinov, V.S. Khabarov, Y.T. Kiryushin, V.S. Kisselev,
I.A. Savin, G.I. Smirnov, D.A. Smolin, J. Strachota, G. Sultanov, P. Todorov, I. Veress,
A.G. Volodko and A.V. Zarubin

JINR, Dubna, USSR

D. Jamnik, R. Kopp, U. Meyer-Berkhout, K.M. Teichert, R. Tirler, R. Voss and Č. Zupančič

Sektion Physik der Universität, Munich, Fed. Rep. Germany

M. Cribier, J. Feltesse, J.P. Fournier, J.C. Michau, A. Milsztajn, A. Ouraou, J.F. Renardy,
P. Rich-Hennion, B. Rothan, Y. Sacquin, G. Smadja, P. Verrecchia and M. Virchaux

CEN, Saclay, France

ABSTRACT

A large toroidal iron spectrometer for the study of deep-inelastic muon scattering at the CERN SPS has been upgraded to extend the accessible kinematic range and to reduce the systematic errors on absolute cross-section measurements. The layout of the improved apparatus, the construction of new detectors and associated electronics, and the structure of a new data-acquisition system are described in detail.

(Submitted to Nuclear Instruments and Methods in Physics Research)

1. INTRODUCTION

The large toroidal spectrometer already used at the CERN SPS muon beam to investigate the deep-inelastic scattering process

$$\mu^{\pm} + N \rightarrow \mu^{\pm} + \text{anything} \qquad (1)$$

has been modified and upgraded with new detectors.

In its original configuration, described in detail in ref. 1, the spectrometer was designed to study the process (1) at large Q^2 with high luminosity, by measuring the momenta and directions of incident and scattered muons. It consisted of 10 identical magnetized iron toroids, 5 m long and 2.75 m in diameter, called "supermodules" (SMs), each equipped with two planes of scintillation counters and eight planes of multiwire proportional chambers (MWPCs). Eight target sections of 5 m length were mounted in the central bores of the SMs, which coincided with the beam axis. The track of the incoming beam muon was recorded in a set of 3 beam hodoscopes in front of the first, third, and sixth targets. The track of the scattered muon, an oscillation in the scattering plane damped by the energy loss in iron, was measured by the MWPCs in two orthogonal projections.

This apparatus has been in operation with a carbon target (isoscalar) during the years 1978–80 to measure the nucleon structure function $F_2^N(x,Q^2)$ [2], the interference between electromagnetic and weak interaction in the deep-inelastic scattering process (1) [3], and the production of events with two muons in the final state [4].

Several years of operating experience, the changeover to a new target (liquid hydrogen), and the evolution of theoretical insight into the scattering process (1) have prevailed on us to embark on a major upgrading of this set-up, mainly in order to measure, with high precision, the proton structure function $F_2^p(x,Q^2)$ at several beam energies. This will allow us to measure the ratio $R = \sigma_L/\sigma_T$ of absorption cross-sections for longitudinally to transversely polarized virtual photons, to study the pattern of scaling violation, and to determine the mass-scale parameter Λ_{QCD} of Quantum Chromodynamics.

These physics aims fix the guidelines for modifications to the apparatus.

i) The apparatus has to operate at high beam intensities (typically 5×10^7 muons per 2 s SPS pulse) with good triggering selectivity and minimal background to accumulate a large number of events in reasonable running times.

ii) The measurement of R is particularly difficult because it requires, at fixed points in the kinematic (e.g. Q^2, x) plane, the comparison of absolute cross-sections measured at different incoming beam energies, and therefore at different times and with different systematic errors. Stringent requirements on the detector for such a measurement are a good overlap between the acceptance regions for the different beam energies, high and uniform triggering and reconstruction efficiencies over a wide kinematic range, and precise counting of the incoming beam particles.

iii) A wide kinematic range is equally important for a study of scaling violation. For the measurement of Λ_{QCD} in particular, a range as wide as possible in log Q^2 is more important than good acceptance at large Q^2 only.

Consequently, the upgrading of the detector concentrated on the following three major items:

i) A small-angle spectrometer at the front end of the apparatus extends the accessible domain of the apparatus described in ref. 1 ($Q^2 \geq 25$ GeV^2 and $x \geq 0.3$), towards smaller Q^2 and x. The

price to pay for this is the removal of two SMs owing to the limited space available in the experimental hall.

ii) Additional plastic scintillation trigger counters of a design different from the earlier ones reduce the sensitivity to background triggers from hadronic showers and enhance, in conjunction with redesigned triggering electronics, the redundancy of the trigger decision, especially in the extended part of the kinematic plane.

iii) A new second-level triggering system requires the presence of a minimal track pattern in the MWPCs before an event is accepted for recording on tape. This system exploits the high redundancy of the track measurement, which was already a quality of the spectrometer in its initial configuration.

These new components of the apparatus are described in detail in sections 2 to 4. In section 5 the largely redesigned data-acquisition system of our experiment is discussed. For a description of all parts of the apparatus which are used without modifications — i.e. magnet, liquid-scintillator trigger counters and MWPCs installed on the SMs, and beam hodoscopes — we refer the reader to ref. 1.

2. LAYOUT OF THE APPARATUS

Figure 1 shows the spectrometer in the new configuration. It consists of

i) the beam- and halo-detection system;

ii) eight SMs which form the toroidal spectrometer;

iii) the new small-angle spectrometer.

2.1 Beam and halo detection system

The two hodoscopes H5 and H6, located upstream of the first target, detect the incoming muon. They have a mosaic structure with 72 counters arranged in concentric rings [1]. The hodoscope H6 defines the useful beam while the hodoscope H5 serves the purpose of measuring, together with H6, the trajectory of the incoming muon. Three additional hodoscopes are installed in the apparatus: H7 between the MWPCs of the small-angle spectrometer and H8 between the last two SMs measure the beam phase space; H9, located $\sim$ 20 m downstream from the last SM behind a 1.5 m long iron absorber, tags the non-interacting muons and is useful in resolving ambiguities in the identification of the beam muon which generated the event.

Halo particles are detected by the "halo wall", a set of veto counters covering a surface of $\sim$ 22 m^2. This system is essentially the same as that described in ref. 1. A set of iron blocks shields the halo wall against back-scattered particles from deep-inelastic scattering in the near target. A new 2.5 m^2 plane of counters, installed 40 m upstream of the experiment, detects a halo component which enters the spectrometer through the central hole of the halo wall.

2.2 Magnetized iron spectrometer

The eight SMs which are in operation are instrumented with the same ring scintillator counters and MWPCs as described in ref. 1. Each SM (fig. 2) has been upgraded with an additional trigger plane made of plastic scintillator counters (section 3.1). They compensate for the dead regions in the old liquid scintillator counters [1] and, being well shielded by the iron disks of the magnet,

reduce the sensitivity to background triggers from hadronic showers (section 4.3). Moreover, they improve the measurement of the time of flight of the scattered muon, needed for the identification of the beam muon which interacted.

The first six SMs are equipped with liquid-hydrogen targets 4.85 m long and 15 cm in diameter, for good containment of the beam over the whole distance from H6 to the last target ($\sim$ 50 m). Lead shields, 4 cm thick, in front of the first trigger counter plane of each SM, reduce by a factor of $\sim$ 2 the rate of triggers from soft electromagnetic and hadronic background.

2.3 Small-angle spectrometer

Two liquid-hydrogen targets (front targets) identical to those mounted on the SMs, have been installed in the upstream end of a 17 m long space made available at the front of the experiment. They are followed by a set of MWPCs (section 3.2) to measure the track of the scattered muons both for precise determination of the scattering angle and of the interaction vertex in hydrogen. The distribution of the interaction vertices along the beam is shown for the front targets and 200 GeV beam in fig. 2a for a hydrogen fill and in fig. 2b for targets empty. The latter plot indicates the concentration of matter in the beam (H6 and target walls).

To cope with the high multiplicity of hadronic showers from deep-inelastic interactions—enhanced by secondary interactions in the 10 m long target—the track measurement was made highly redundant by installing seven consecutive chambers, each equipped to measure three projections. The efficiency in identifying unambiguously the correct muon trajectory is somewhat dependent on the scattering angle and the kinematic cuts, but is in any case larger than 90%. Muons scattered off the front targets travel on average 12 m before entering the iron spectrometer for triggering and momentum measurement; the minimum scattering angle is 15 mrad.

Acceptance contours of the spectrometer for muons scattered from the front targets and from the targets in the SMs are compared in fig. 4. It is clearly seen that the small-angle spectrometer does not only enlarge the kinematic range of the apparatus, in particular at low beam energies, but also improves greatly the overlap of the acceptance regions for different beam energies.

3. NEW DETECTORS

3.1 Trigger counters

Eight identical planes of mosaic trigger counters, one per SM, have been constructed. Each plane consists of 20 trapezoidal counters I1–I8 and O1–O12 (see fig. 5), disposed in two concentric rings around the beam axis. For a good overlap between the elements of a plane, the counters have been inserted in different slits of the magnet iron (see fig. 2); the maximum distance along the beam direction between two counters of the same plane is 60 cm. The planes cover a surface of 2.75 m external and 0.56 m internal diameter. The dimensions of the scintillators are 74 cm, 26 cm (the two bases), and 58 cm (the trapeze height), for the inner ring counters I1–I8, and 74 cm, 40.5 cm, and 63 cm, respectively, for the outer O1–O12 elements. The counters are made of 1 cm thick NE 110 scintillator viewed by a 2-inch fast photomultiplier EMI 9814KB.

The matching of a 74 $\times$ 1 cm^2 scintillator area to a 2 inch diameter photocathode requires optimized light-guides. The design of the light-guides was constrained by various mechanical obstructions around the iron toroids, such as coils, supports, etc., which required the construction of four different shapes. Apart from counters I4 and I5, which are seen through a side, the other

counters are seen via adiabatic light-guides, 56 × 1 cm^2, from the wider base of the trapeze. The matching between the outer side of the counter and the light-guide is made with a rectangular plate of plexiglas which disperses the light over a wide area. The adiabatic light-guides have been manufactured using the technique of laser cutting*).

The other three narrow sides of the counter are painted black to avoid light reflections which would widen the light pulse or cause multiple PM pulses. The counter prototypes have been extensively checked in a test beam in order to measure their efficiency and the dependence of pulse height on the point where the particle traverses the scintillator. The average number of photoelectrons varies between 10 and 30 for the worst counter. The problem of reducing after-pulsing and at the same time keeping a reasonably narrow pulse shape from the PM has been solved by clipping and slightly integrating the anode pulse with a passive circuit connected to the PM anode.

3.2 Hexagonal three-coordinate proportional chambers

The seven MWPCs in the small-angle spectrometer are of hexagonal shape, each of them containing 3 planes of sense wires rotated by 60° with respect to each other. Two types of chamber have been made, which differ in size, wire pitch, and construction technique. The first five chambers have a sensitive region of 1.5 m diameter and a wire pitch of 2 mm, while for the last two larger chambers these figures are 2.11 m and 3 mm, respectively.

The five small hexagonal chambers have been built with self-supporting HV planes made of 20 mm thick honeycomb panels sandwiched, for rigidity, between two 250 μm thick layers of vetronite. The panel sides, coated with a conductive silver paint, are the HV cathodes. This technique has been successfully employed for the construction of the 128 MWPCs installed in the SMs [1]. Figure 6 shows an exploded view of a chamber. The HV planes are divided by a 2 mm gap in the silver paint into two concentric parts connected to separate HV power supplies. The central region, which is exposed to the beam, is 10 cm in diameter, and is normally operated with a HV reduced with respect to the outer cathode to withstand the high flux at the expense of a low efficiency for beam particles. At low intensity, the central region may be operated at full efficiency to measure the phase space of the beam with good resolution.

The sense wires are made of 20 μm gold-plated tungsten wires soldered on printed circuits, which in turn are glued on the honeycomb panels.

Two supporting wires keep the sense wires in place, and three spacers maintain a constant 14 mm cathode-to-cathode gap. The chamber frames, made of vetronite, are held together by 42 dowels and made gas-tight by three soft O-rings (fig. 7).

The two large chambers are of a more classical design: the wire planes, as well as the HV planes, are held in place by a thick aluminium frame. The wire pitch is 3 mm, and the cathode-to-cathode gap is 12 mm. The sense wires are kept aligned by "garlands" [5] laid between the wire and HV planes. A 1 kV voltage applied to the conductive core of the garlands minimizes the insensitive regions around them. The HV planes are made of mylar sheets coated with graphite and are also divided in two HV regions, the central one being 20 cm in diameter.

---

*) Société technique de réalisations industrielles, Suresnes, France.

4. TRIGGER

The principle of the distributed trigger [1] was retained for the new spectrometer layout. Briefly, it requires events of a minimum track length (controlled by the minimum number of consecutive trigger counter planes) and a minimum sagitta (controlled by the radius of rings activated in the liquid scintillator counters), occurring anywhere along the target. For events from the targets in the SMs, these requirements correspond to minimum values of the transverse momentum p_T and of the four-momentum transfer Q^2 of the scattered muon, respectively. The same trigger requirements are applied to tracks from the small-angle spectrometer entering the SMs from the front, although the simple correspondence between geometric and kinematic variables is lost for this type of event. Halo triggers were suppressed by requiring a coincidence with the beam signal and using the signal from the halo wall in anticoincidence.

4.1 First-level trigger

Even if the basic principles of the fast first-level triggering system remained unchanged, it was improved in several respects:

i) More versatile coincidence matrices [6], one in each SM except the first, allow a maximum of 12 coincidence combinations to be selected simultaneously out of 8 inputs. These are connected to the output signals of the three trigger counter planes in the respective SM, plus the signals of three planes upstream and two planes downstream (fig. 8). The 12 coincidence signals, after validation by the (beam · anti-halo) signal, are ORed to form the first-level trigger. The basic trigger requirement is that a track traverses six consecutive trigger counter planes, but one out of the six plane signals may be missing. This allows for some detection inefficiency, in particular for the effect of the spacer bars which separate the rings of the liquid scintillator counters [1]. At least one new plane is always required to reduce the sensitivity of the trigger to hadronic shower background. This scheme is to be compared with the earlier one which required at least four consecutive planes—corresponding to about the same track length because of the larger distance between the counters—and thus provided a limited redundancy only for long tracks traversing at least five planes.

ii) The apparatus was logically split into two halves by forming all plane and coincidence signals separately for the left and the right side of the counter planes. This reduces the number of shower triggers and allows the imposition of additional constraints on the second-level trigger (section 4.2).

iii) The "highway" network of fast air-core cables was largely restructured. This system which carries all counter, beam, and trigger signals, interconnects the SMs at almost the speed of light to preserve synchronization between the muon traversing the spectrometer and all trigger signals, albeit with a fixed delay. Several rearrangements permit better exploitation of the maximum allowed propagation time through the trigger system between the traversal of a particle and the arrival of a strobe signal at the MWPC electronics mounted on the chambers themselves; this time is limited by the MWPC monostable delay and amounts to $\sim$ 470 ns. The faster generation of the trigger permits all chambers to be strobed in time up to 15 m upstream of the first triggering plane. This facilitates the identification of background, from halo tracks which enter the spectrometer from the front but give a trigger only a few SMs downstream.

All the first-level electronics is computer-controlled via the SATAN system already described in ref. 1.

4.2 Second-level trigger

In order to reduce further the contribution of background triggers from hadronic showers, a filtering system was developed which requires that an indication of a track is seen in the MWPCs installed on the SMs to validate an event. The outputs of the memory ORs of each chamber (MOR) are sent to four CAMAC-controlled processors, one for each type of chamber (top, bottom, left, right), which compare the hit pattern of the event with a predefined reference pattern. A choice of such patterns is stored in field-programmable logic arrays (FPLAs) and one of them is actually selected for triggering by CAMAC control. These patterns are all of the type that they require n out of $m \geq n$ consecutive chambers anywhere in the apparatus to be hit, with $4 \leq n,m \leq 6$.

A similar CAMAC module processes the first-level trigger information and allows it to be compared with the MWPC pattern. It uses the output of the coincidence matrices to decide in which SM and on which side (left/right) of the spectrometer the first-level trigger occurred. Signals from the new trigger counters can be used to identify the corresponding quadrant (left-bottom, right-top, etc.). Additional requirements may then be imposed on the final trigger decision, such as a maximum distance between the MWPC track and the first triggering SM in the beam direction, or compatibility between the sides (or quadrants) of the trigger and of the MWPCs.

Upon final validation of an event, the logic pattern of all input signals to the second-level trigger is recorded by the on-line computer to monitor continuously the performance of the system.

4.3 The beam · anti-halo signal and beam counting

An accurate counting of those muons which can trigger the apparatus is needed for measuring the absolute cross-section. In order to have a reliable measurement of the beam flux the halo anticoincidence has been applied to the beam signal prior to counting. Therefore, the signals of individual channels of the beam-defining hodoscope H6 are sent to shapers with a common veto input driven by the halo signal. The beam · anti-halo pulse is the OR of the inner 48 cells of H6, covering a surface of $\sim$ 8.4 cm diameter.

The electronics used to generate the beam trigger signal and to count the incoming beam flux operates at frequencies $\geq$ 200 MHz — including the counting of individual hodoscope channels for an independent flux measurement — to minimize counting losses. The "beam" signal—from the OR to the scaler—is counted with $\sim$ 300 MHz electronics.

4.4 Trigger rates

The upgrading of the triggering electronics and other measures taken to reduce the various sources of background allow operation of the experiment routinely at beam intensities up to 5×10^7 muons per SPS spill; data are taken including all rings of the liquid scintillator counters in the trigger, thus exploiting fully the Q^2 range of the spectrometer. The first-level trigger rates, after the first-level decision which strobes all MWPCs and CAMAC modules, are 1.2×10^{-4}, 7.5×10^{-5}, and 3×10^{-5} for 280, 200, and 120 GeV beam energy, respectively.

In standard data-taking mode, the second-level trigger requires four out of six consecutive chambers, where the two missing chambers must not follow each other immediately. In addition, the four chambers hit must be on the same side of the spectrometer where the first-level trigger

occurred. These requirements cut down the first-level trigger rate by a factor 10–20, depending on the beam energy. More stringent requirements on the geometric compatibility between first- and second-level trigger do not result in an appreciable further reduction.

Typical trigger rates are 2.5×10^{-6}, 5×10^{-6}, and 8×10^{-6} for 120, 200, and 280 GeV beam energy. In practice, this corresponds to 100–200 triggers per 2 s SPS spill since very high intensities are normally not available with the top energy of 280 GeV. Still, the trigger composition is dominated by background from hadronic showers and halo feedthrough and the fraction of good deep-inelastic events varies from 50% at the lowest to 10% at the highest beam energy.

5. DATA ACQUISITION

5.1 On-line computers and CAMAC systems

Three Norsk Data processors are used in the experiment (fig. 9): a Nord-100 configuration with 768 kbytes memory and a 10 Mbytes disk, a Nord–10S with 512 kbytes memory and a 66 Mbytes disk, and a Nord–50 32-bit processor unit coupled to the Nord–10 and sharing its memory through multiport access. The Nord–100 is dedicated to data taking, while the Nord–10 system is used for hardware tests and remote electronics control. NORDNET communications software links the machines via an RS232 9600-baud line and is used for remote terminal log-in and exchange of program and data files. The ND–10S system is connected to the CERNET [7] network using standard CAMAC modules for access to the CDC and IBM main-frame computers of the CERN computing centre.

The data acquisition is based on a CAMAC system interfaced to the on-line computers by Norsk Data system crates [8]. The read-out of the experimental data was converted to the fast CERN-designed REMUS system [9], subdivided into six branches (fig. 10). The tree structure of the REMUS system allows an individual addressing of each branch according to the type of trigger. Via a REMUS routing unit, events can be read from the Nord–10 and/or the Nord–100. An additional CAMAC branch, accessible from both computers via a branch mixer, accommodates control modules for remote electronics, TV display drivers, an SPS data interface, etc. A flexible, CAMAC-controlled trigger-processing unit has been developed which allows several types of monitoring and test triggers to run simultaneously and enables, for each type of trigger, the relevant REMUS branches, both outside SPS bursts or concurrent with the physics trigger.

The software used is based on the CERN-written program package DAS [10], a modular Data Acquisition System designed as a set of independent tasks which communicate via a structured common data area and a message system. Our implementation runs on both machines under control of the Norsk Data SINTRAN III real-time operating system. Sixteen hardware interrupt levels—each with its own set of hardware registers—allow interrupt driven tasks to bypass the operating system, making the acquisition fast and efficient. This feature has been used for the CAMAC/REMUS read-out and tape writing tasks. Multi-tasking makes the system very modular since tasks may be freely added when the need arises and can be started, suspended, or aborted during data taking. On-line analysis is performed by independent programs (tasks) whose size ranges from a few kbytes for simple tasks up to nearly 128 kbytes for complex monitoring programs. The present configuration handles eight "event consumer" tasks dedicated to the analysis of different parts of the spectrometer. All tasks are written in FORTRAN 77 and use common libraries to communicate with their environment, such as raw-event data, data blocks from

other tasks, parameters, messages, etc. Most of these tasks produce output in the form of histograms for visual inspection on graphics terminals.

The data-acquisition dead-time of the experiment is determined by the CAMAC cycle time for Direct Memory Access (DMA) transfers, which is 1.8 μs per 16-bit word for REMUS read-out, and by the software overhead of 800 μs per event for interrupt handling, DMA preparation, event buffer handling, etc. For an average of 130 events, each about 900 bytes long, per effective SPS spill of 1.5 s, this corresponds to a dead-time of $\sim$ 15%.

5.2 On-line monitoring

To extend the monitoring capabilities of the on-line system beyond the analysis based on physics events, a powerful test-event system verifies continuously the performance of all detectors, and of the triggering and data-acquisition systems. Test pulses are generated by computer programs and travel along the experiment via a dedicated highway to simulate the passage of a muon track. They are fanned out to the MWPCs to test the functioning of all read-out channels and to light-emitting diodes (LEDs) in the trigger counters to monitor the stability of both pulse height and timing of the photomultipliers with ADCs and TDCs respectively. A suitable design of the remotely controlled fan-outs allows the LEDs to be flashed with various logic patterns in order to test in detail all possible coincidence combinations of the trigger system. For routine tests during normal data taking, the system is fully automatic and the test programs are scheduled for execution on the Nord–10 computer in $\sim$ 15 min intervals.

6. CONCLUSIONS

The apparatus described above has a flat and high acceptance in a wide x and Q^2 domain. The cut-off values of x and Q^2 for 45% acceptance are at 0.05 and 10 GeV^2, respectively, in the energy region available at the CERN SPS. This represents a considerable extension of the domain which was accessible for the structure-function measurements with the original spectrometer [1], i.e. $x \geq 0.3$ and $Q^2 \geq 25$ GeV^2. The apparatus in its upgraded form has been in operation since the beginning of 1982 and all its components have proved to work reliably. So far, data were taken mainly for the measurement of the proton structure function at beam energies of 100, 120, 200, and 280 GeV.

The distributed target layout and the possibility to fill the target vessels with liquids other than hydrogen make our spectrometer particularly well-suited for simultaneous measurements of the deep-inelastic cross-section with different target materials and small systematic errors. This feature is of great interest after the discovery of a nuclear effect in the x dependence of the structure function F_2 [11], and data have been taken recently with combinations of deuterium/iron and nitrogen/iron targets.

Acknowledgements

The improvement of our spectrometer would not have been possible without the technical support of CERN and our home laboratories, in particular the skilful work of K. Bussman, H. Herbert, P. Klemm, P. Marelli, G. Miller, V. Vishnevsky and H. Willaredt. We are particularly grateful to V. Evdokimov, G. Molinari, R. Pilastrini, N. Shcherbakov, L. Svetov and Y. Zlobin for

their excellent work done during the commissioning of the new MWPCs and trigger counters. The enthusiastic work of H. Arandel, L. Briot, C. Gregory, L. Mazzone and B. Vuillierme on the construction, installation, and operation of the large and delicate liquid-hydrogen target is greatly appreciated. Finally, we wish to thank all the physicists who have contributed to the upgrading programme, especially J. Cvach, N. Fadeev, A. Kondor, W.D. Nowak, G. Vesztergombi, S. Vorozhtsov and J. Zacek.

REFERENCES

[1] D. Bollini et al., Nucl. Instrum. Methods **204** (1983) 333.
[2] D. Bollini et al., Phys. Lett. **104B** (1981) 403.
[3] A. Argento et al., Phys. Lett. **120B** (1983) 245.
[4] D. Bollini et al., Nucl. Phys. **B199** (1982) 27.
[5] S. Majewski and F. Sauli, CERN NP Internal Report 75–14 (1975).
[6] G.F. Nanni, CERN–EP Internal Report 81–11 (1981).
[7] J.M. Gerard (ed.), CERN 81–12 (1981).
[8] J.P. Vanuxem, CERN CAMAC Note 60–01, 1978.
[9] P. Ponting, CERN/EP Electronics Note 80–01, 1980.
[10] A. Bogaerts, M. Dehnert and J. Petersen, DAS Reference manual, CERN DD/OC/ ND/81–2, 1981.
[11] EMC Collaboration, J.J. Aubert et al., Phys. Lett. **123B** (1983) 275.

Figure captions

Fig. 1 : Layout of the upgraded spectrometer.

Fig. 2 : Side view of a magnetic iron toroid (SM).

Fig. 3 : Distribution of the z coordinate of reconstructed interaction vertices in the front targets, for 200 GeV data with (a) full and (b) empty targets.

Fig. 4 : Contours of 45% acceptance for beam energies of (a) 100 GeV and (b) 200 GeV. The solid lines refer to muons detected by the small-angle spectrometer and the dashed lines to events from targets in the SMs.

Fig. 5 : View of the three counter planes which equip one SM, showing in detail the rings and the light-guides of the old counters (only the right side is shown) and the structure of the new counters. The outer counters on the left side and the light-guides of the inner counters on the right side are not shown for clarity.

Fig. 6 : Exploded view of a hexagonal three-coordinate MWPC.

Fig. 7 : Cross-section view of a frame of the hexagonal MWPCs.

Fig. 8 : Simplified block diagram of the fast first-level trigger system. The logic circuit of one SM only is shown in some detail.

Fig. 9 : Configuration of on-line computers and peripherals.

Fig. 10 : Structure of the read-out and experiment control system.

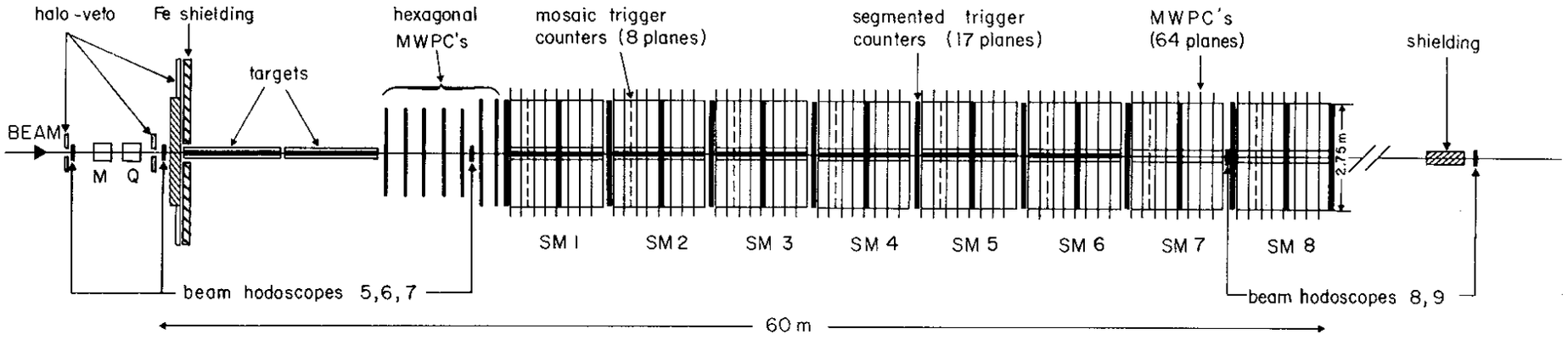
halo-veto
Fe shielding
hexagonal MWPC's
mosaic trigger counters (8 planes)
segmented trigger counters (17 planes)
MWPC's (64 planes)
shielding
targets
BEAM
M
Q
SM 1
SM 2
SM 3
SM 4
SM 5
SM 6
SM 7
SM 8
2.75 m
beam hodoscopes 5,6,7
beam hodoscopes 8,9
60 m

Fig. 1

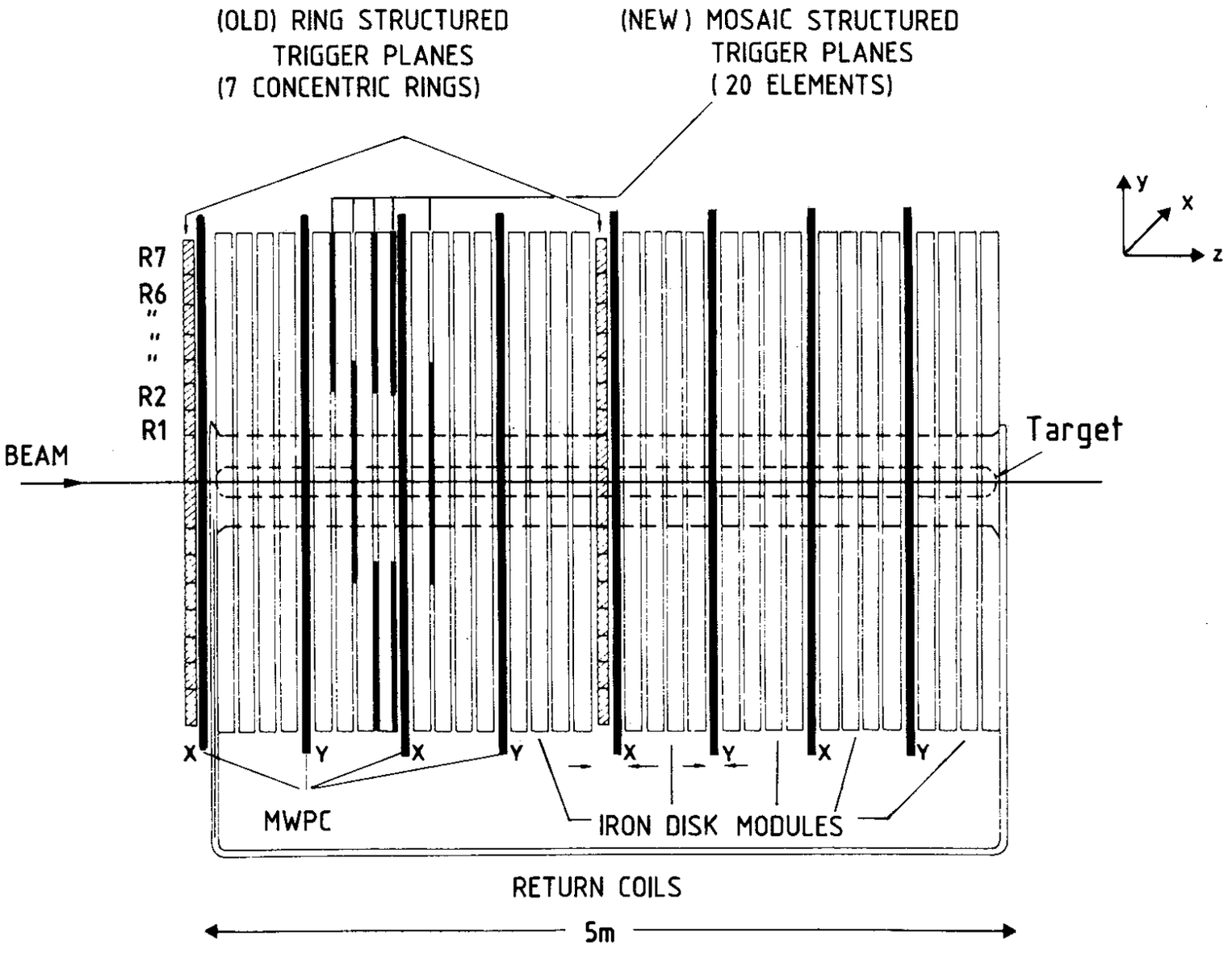
(OLD) RING STRUCTURED
TRIGGER PLANES
(7 CONCENTRIC RINGS)
(NEW) MOSAIC STRUCTURED
TRIGGER PLANES
(20 ELEMENTS)
y
x
z
R7
R6
R2
R1
BEAM
Target
X
Y
X
Y
X
Y
X
Y
MWPC
IRON DISK MODULES
RETURN COILS
5m

Fig. 2

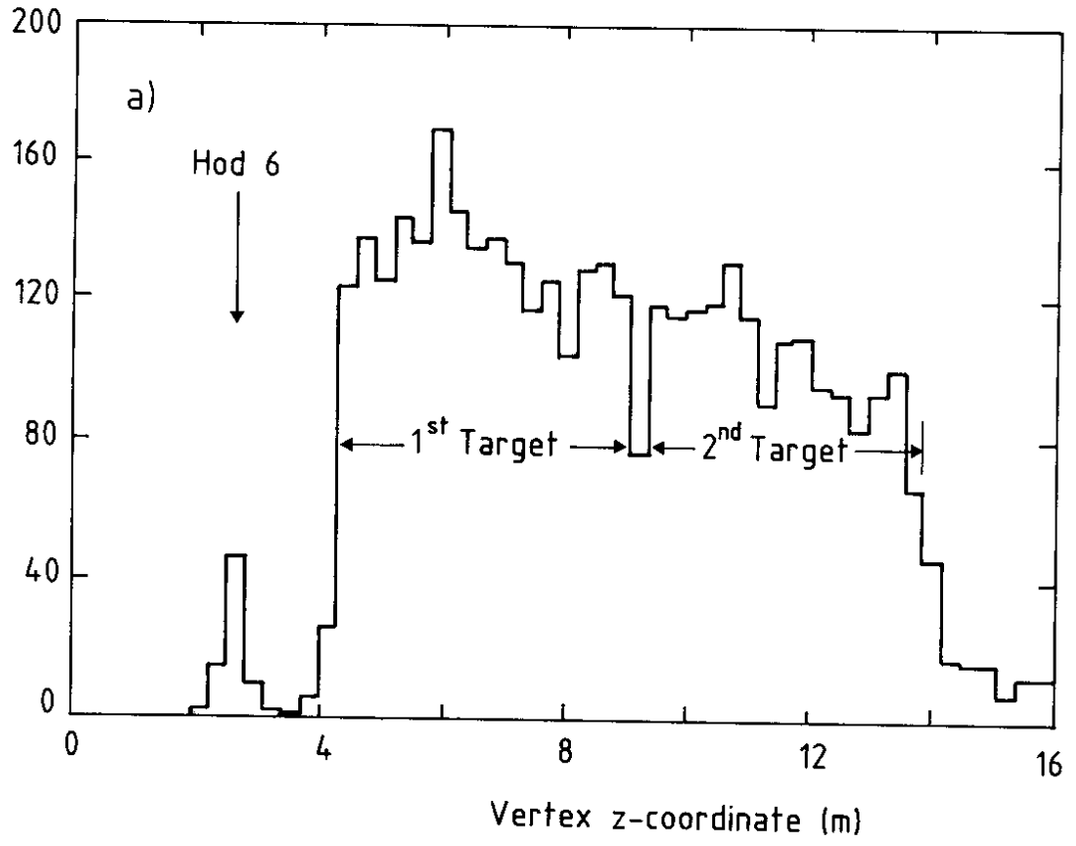
a)
Hod 6
1st Target
2nd Target
200
160
120
80
40
0
0
4
8
12
16
Vertex z-coordinate (m)

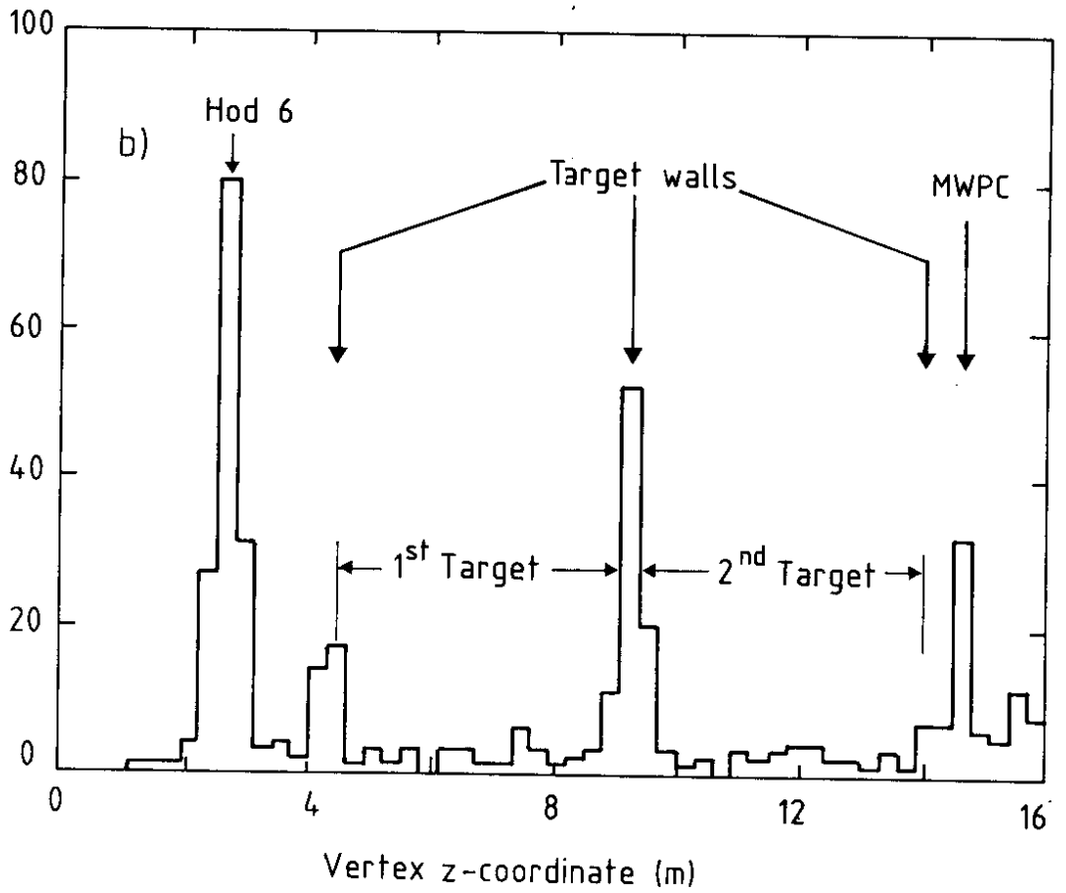
b)
Hod 6
Target walls
MWPC
1st Target
2nd Target
100
80
60
40
20
0
0
4
8
12
16
Vertex z-coordinate (m)

Fig. 3

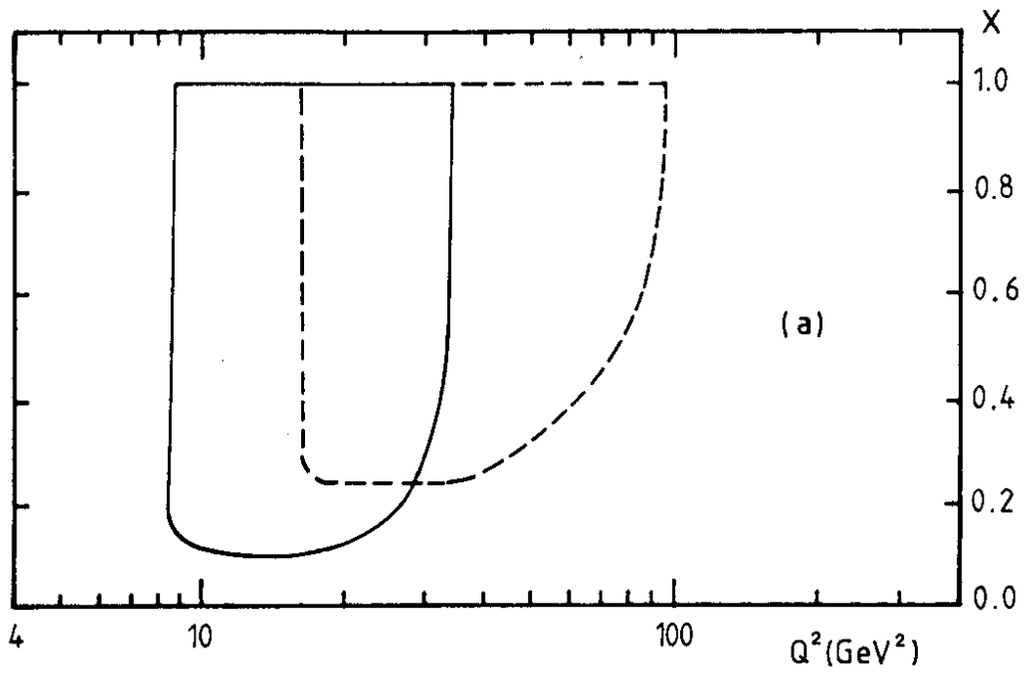
X
1.0
0.8
0.6
0.4
0.2
0.0
(a)
4
10
100
Q²(GeV²)

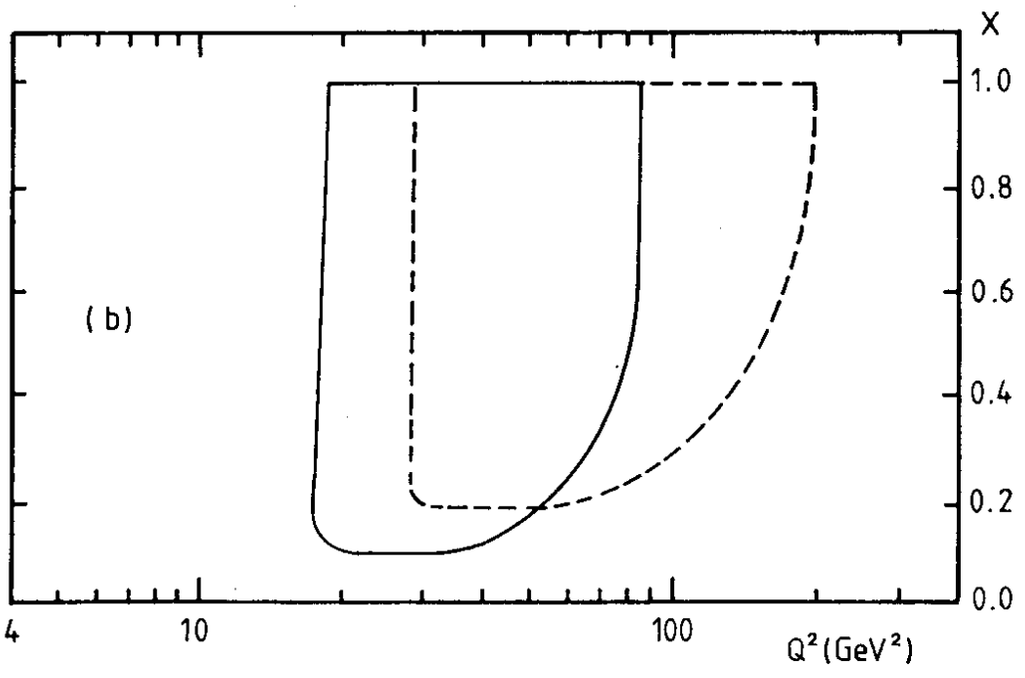
X
1.0
0.8
0.6
0.4
0.2
0.0
(b)
4
10
100
Q²(GeV²)

Fig. 4

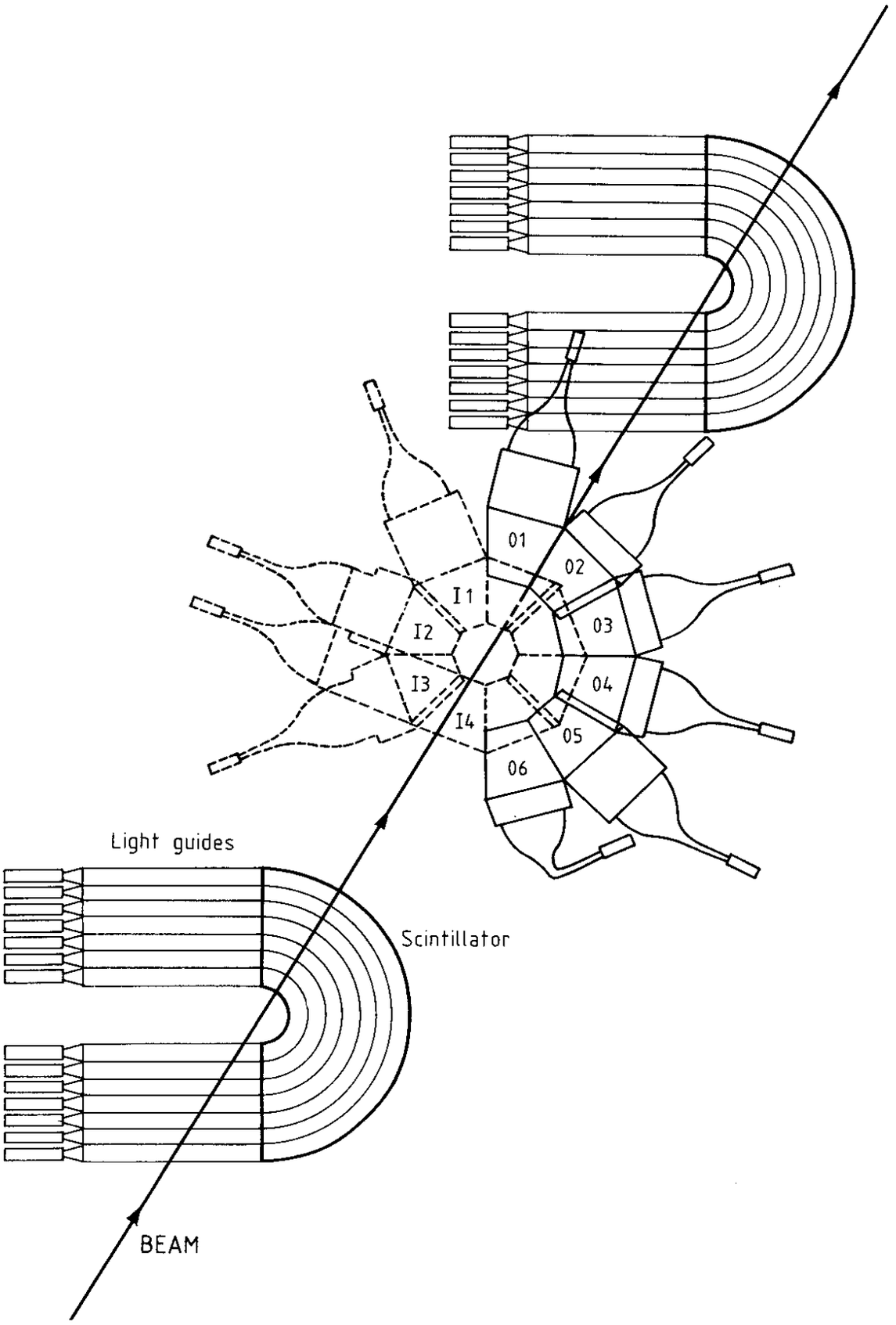

Fig. 5

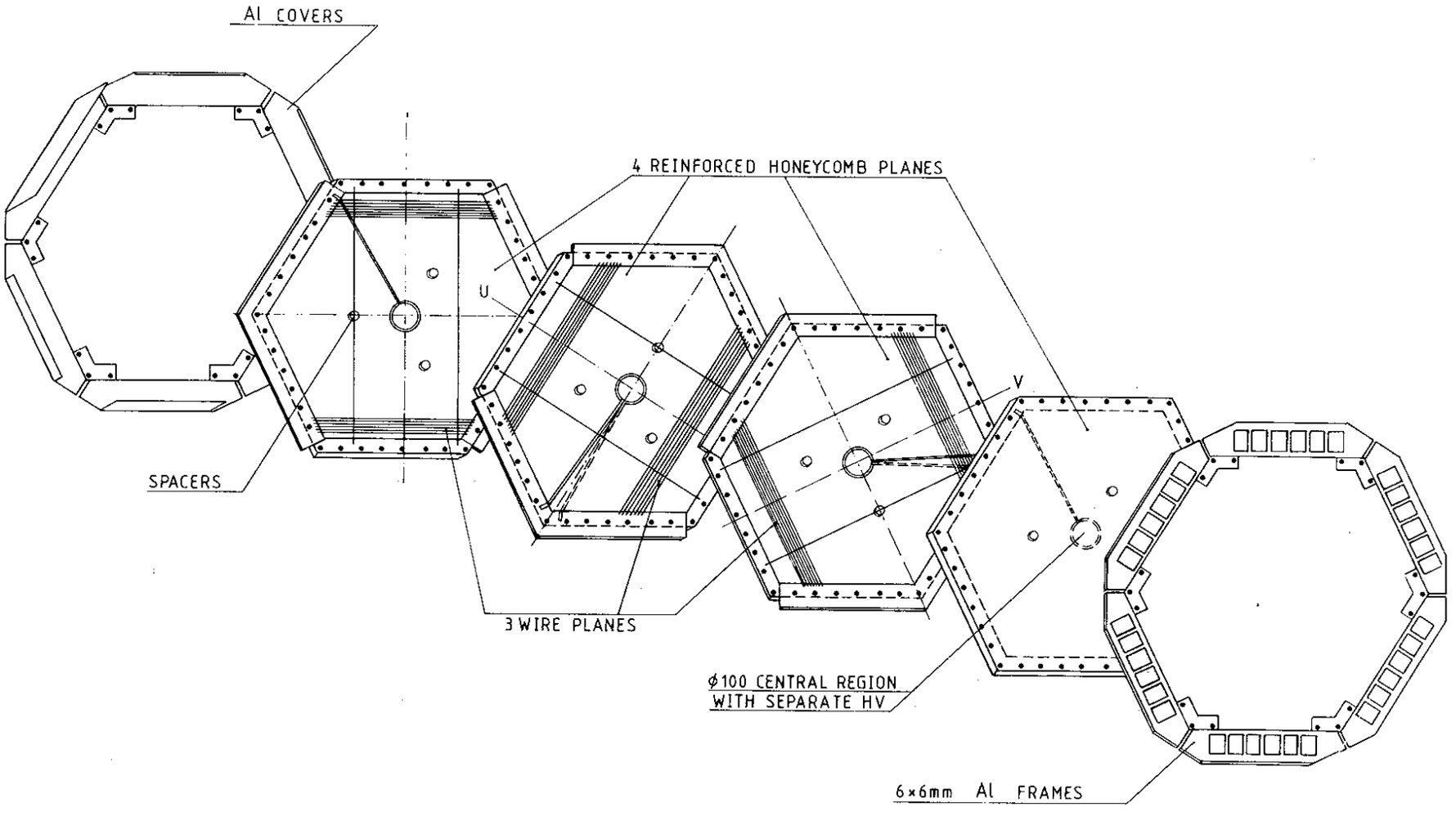
Al COVERS
4 REINFORCED HONEYCOMB PLANES
U
V
SPACERS
3 WIRE PLANES
ϕ100 CENTRAL REGION
WITH SEPARATE HV
6×6mm Al FRAMES

Fig. 6

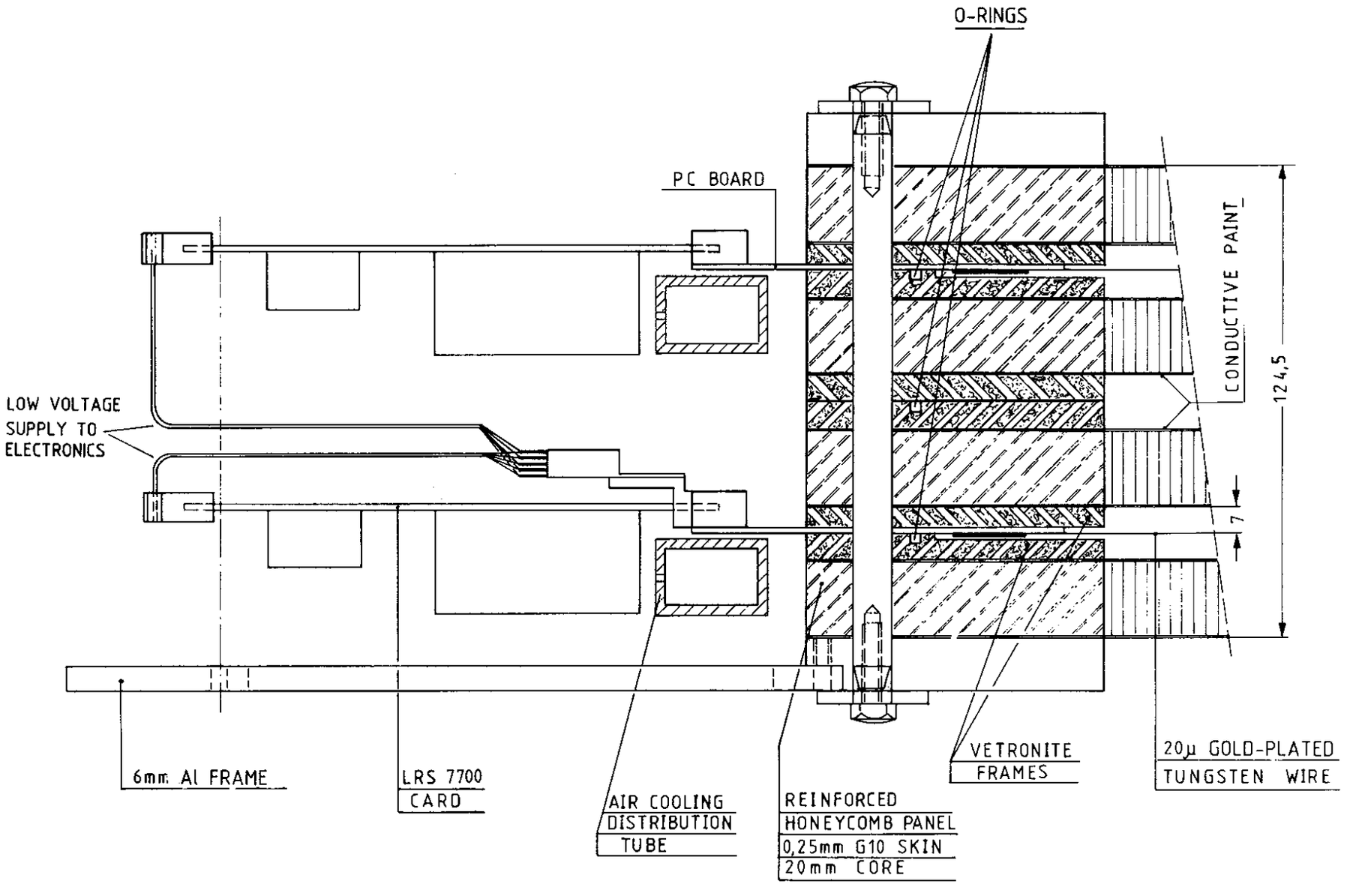
O-RINGS
PC BOARD
CONDUCTIVE PAINT
124,5
7
LOW VOLTAGE
SUPPLY TO
ELECTRONICS
6mm Al FRAME
LRS 7700
CARD
AIR COOLING
DISTRIBUTION
TUBE
REINFORCED
HONEYCOMB PANEL
0,25mm G10 SKIN
20mm CORE
VETRONITE
FRAMES
20µ GOLD-PLATED
TUNGSTEN WIRE

Fig. 7

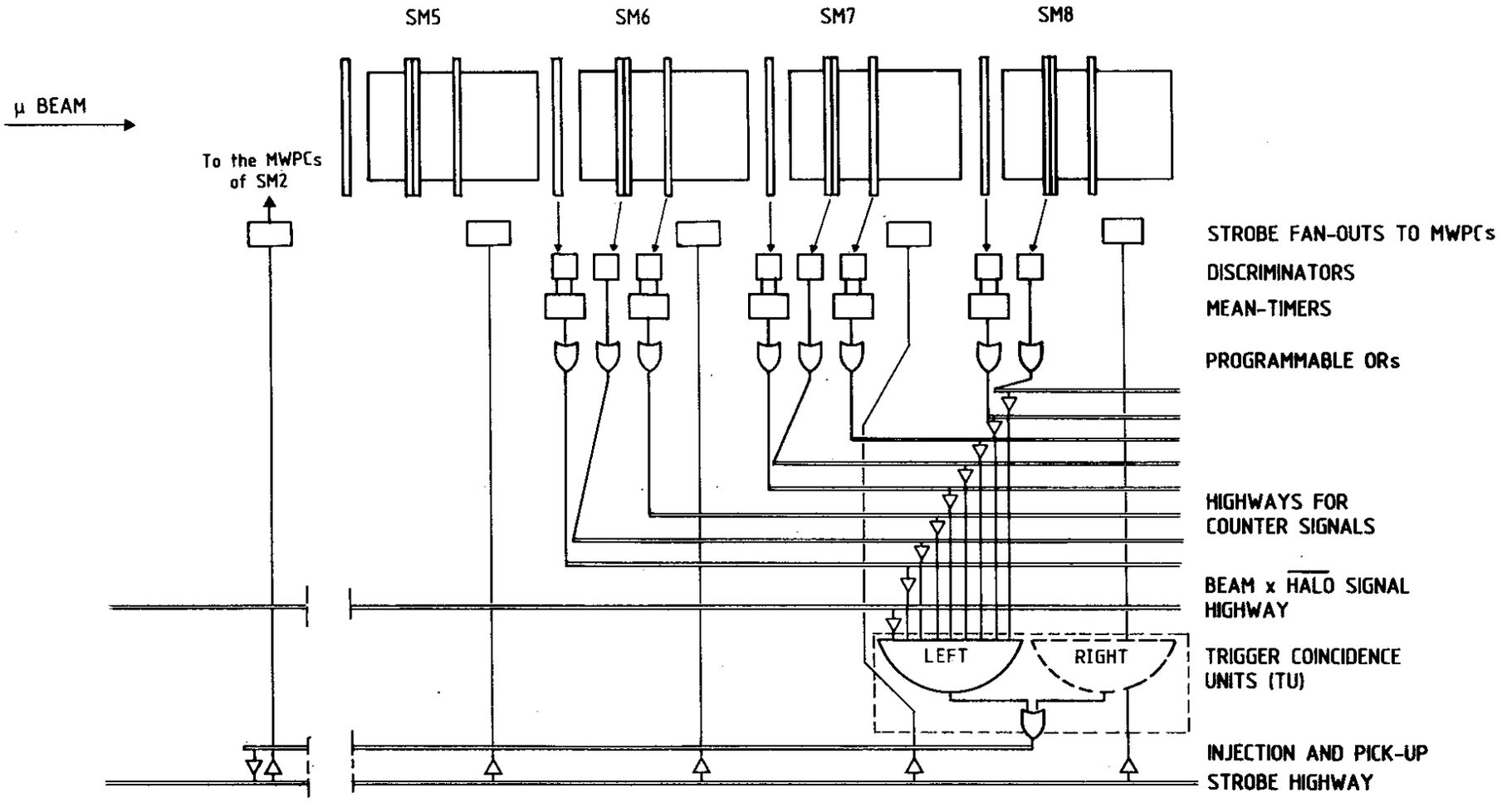
SM5
SM6
SM7
SM8
μ BEAM
To the MWPCs of SM2
STROBE FAN-OUTS TO MWPCs
DISCRIMINATORS
MEAN-TIMERS
PROGRAMMABLE ORs
HIGHWAYS FOR COUNTER SIGNALS
BEAM x $\overline{\text{HALO}}$ SIGNAL HIGHWAY
LEFT
RIGHT
TRIGGER COINCIDENCE UNITS (TU)
INJECTION AND PICK-UP STROBE HIGHWAY

Fig. 8

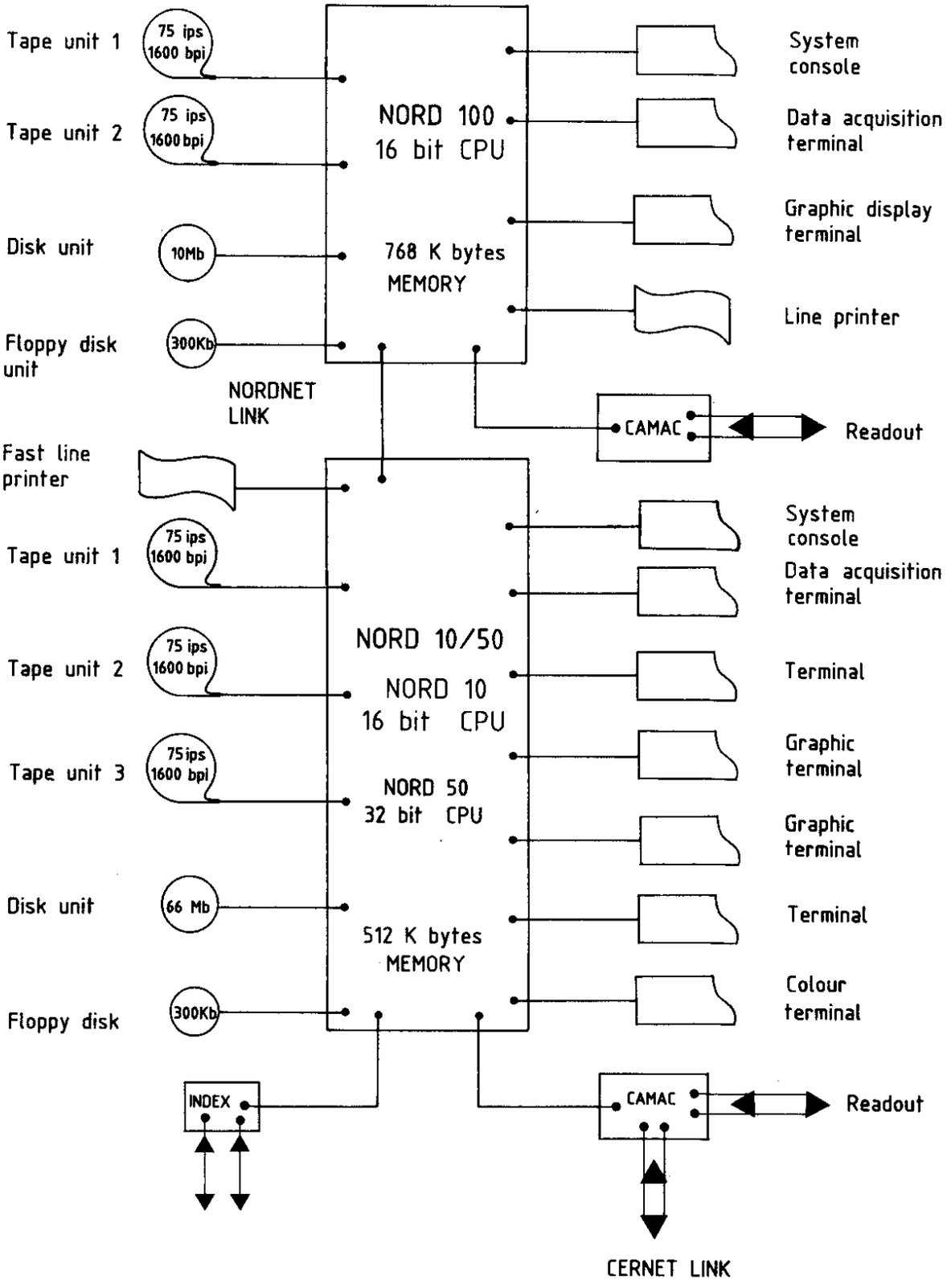
Tape unit 1
75 ips 1600 bpi
Tape unit 2
75 ips 1600 bpi
Disk unit
10Mb
Floppy disk unit
300Kb
NORD 100
16 bit CPU
768 K bytes MEMORY
NORDNET LINK
System console
Data acquisition terminal
Graphic display terminal
Line printer
CAMAC
Readout
Fast line printer
Tape unit 1
75 ips 1600 bpi
Tape unit 2
75 ips 1600 bpi
Tape unit 3
75 ips 1600 bpi
Disk unit
66 Mb
Floppy disk
300Kb
NORD 10/50
NORD 10
16 bit CPU
NORD 50
32 bit CPU
512 K bytes MEMORY
System console
Data acquisition terminal
Terminal
Graphic terminal
Graphic terminal
Terminal
Colour terminal
INDEX
CAMAC
Readout
CERNET LINK

Fig. 9

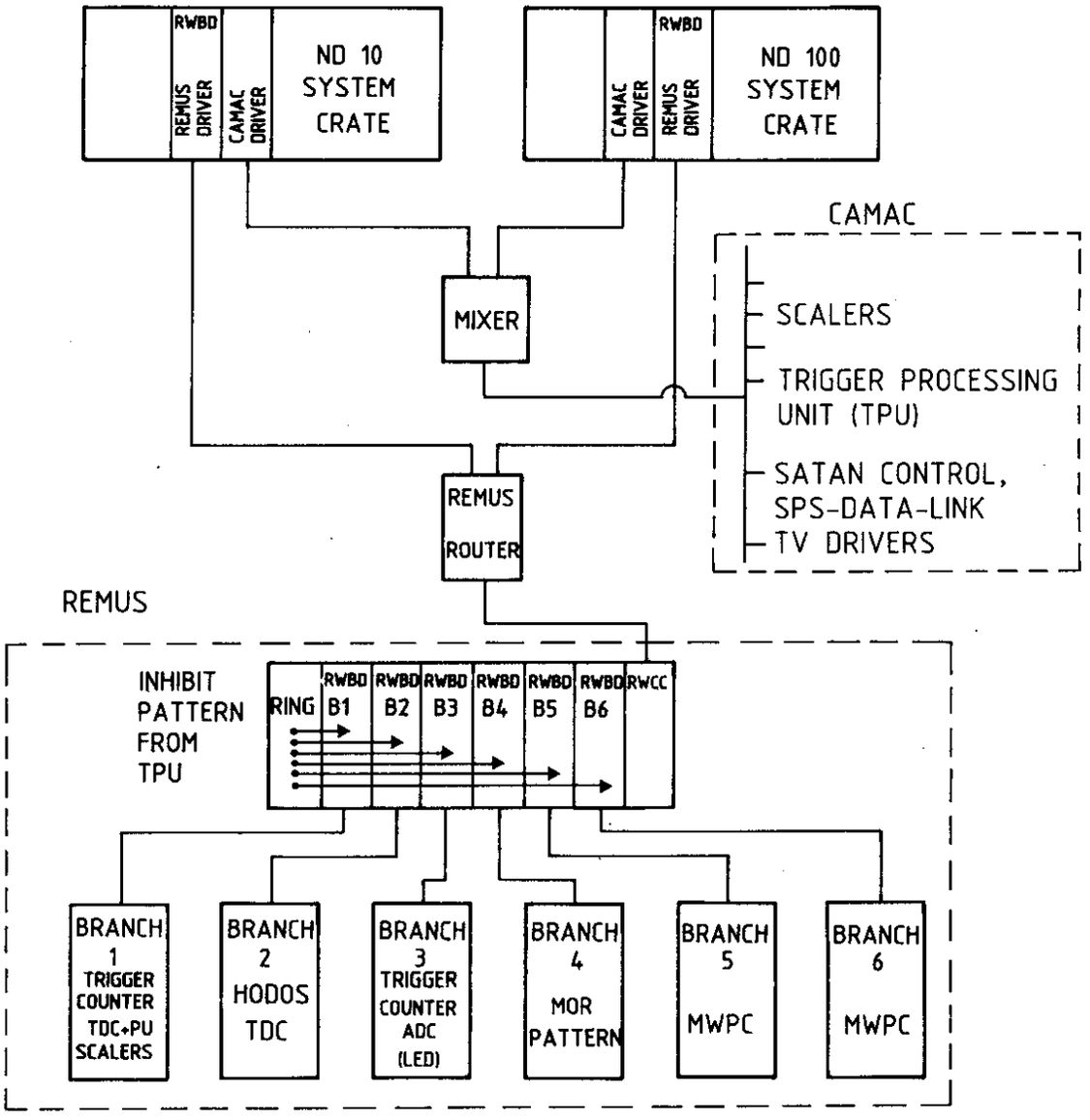
RWBD
REMUS DRIVER
CAMAC DRIVER
ND 10 SYSTEM CRATE
CAMAC DRIVER
RWBD
REMUS DRIVER
ND 100 SYSTEM CRATE
CAMAC
MIXER
SCALERS
TRIGGER PROCESSING UNIT (TPU)
SATAN CONTROL, SPS-DATA-LINK TV DRIVERS
REMUS ROUTER
REMUS
INHIBIT PATTERN FROM TPU
RING
RWBD B1
RWBD B2
RWBD B3
RWBD B4
RWBD B5
RWBD B6
RWCC
BRANCH 1 TRIGGER COUNTER TDC+PU SCALERS
BRANCH 2 HODOS TDC
BRANCH 3 TRIGGER COUNTER ADC (LED)
BRANCH 4 MOR PATTERN
BRANCH 5 MWPC
BRANCH 6 MWPC

Fig. 10